



Published in final edited form as:

Immunity. 2018 May 15; 48(5): 963–978.e4. doi:10.1016/j.immuni.2018.04.017.

Intestinal epithelial Wnt signaling mediates acetylcholine-triggered host defense against infection

Sid Ahmed Labeled^{1,‡}, Khursheed A. Wani[‡], Sakthimala Jagadeesan², Abdul Hakkim², Mehran Najibi^{1,‡}, and Javier Elbio Irazoqui^{1,*}

¹Center for the Study of Inflammatory Bowel Disease, Massachusetts General Hospital Research Institute, Harvard Medical School, Boston, MA 02114

²Department of Molecular Biology, Massachusetts General Hospital Research Institute, Harvard Medical School, Boston, MA 02114

SUMMARY

Regulated antimicrobial peptide expression in the intestinal epithelium is key to defense against infection and to microbiota homeostasis. Understanding the mechanisms that regulate such expression is necessary for understanding immune homeostasis and inflammatory disease, and for developing safe and effective therapies. We used *Caenorhabditis elegans* in a preclinical approach to discover mechanisms of antimicrobial gene expression control in the intestinal epithelium. We found an unexpected role for the cholinergic nervous system. Infection-induced acetylcholine release from neurons stimulated muscarinic signaling in the epithelium, driving downstream induction of Wnt expression in the same tissue. Wnt induction activated the epithelial canonical Wnt pathway, resulting in the expression of C-type lectin and lysozyme genes that enhanced host defense. Furthermore, the muscarinic and Wnt pathways are linked by conserved transcription factors. These results reveal a tight connection between the nervous system and the intestinal epithelium, with important implications for host defense, immune homeostasis, and cancer.

eTOC blurb

How intestinal epithelial antimicrobial defense functions are regulated is poorly understood. Using *Caenorhabditis elegans*, Labeled et al. found infection-triggered neuronal acetylcholine release, driving intestinal defense gene expression via conserved muscarinic and Wnt pathways. This

*Correspondence: javier.irazoqui@umassmed.edu.

‡Present address: Department of Microbiology and Physiological Systems, University of Massachusetts Medical School, Worcester, MA 01605

Lead Contact: Javier E. Irazoqui

Author Contributions

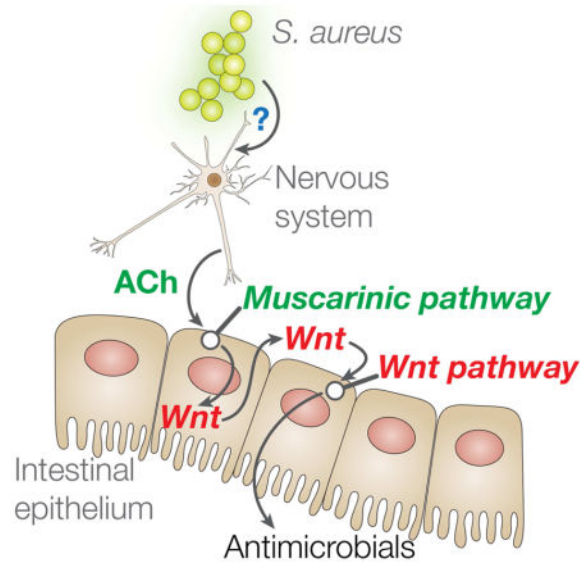
S.L. performed, analyzed, and reported most experiments. K.W. performed aldicarb assays and specific experiments. S.J. and A.H. helped with the RNAi screens. M.N. contributed to specific experiments. J.E.I. provided key intellectual input and overall guidance for experimental design, execution, interpretation, and reporting. All authors contributed to writing the manuscript.

Declaration of interests

The authors declare no competing interests.

Publisher's Disclaimer: This is a PDF file of an unedited manuscript that has been accepted for publication. As a service to our customers we are providing this early version of the manuscript. The manuscript will undergo copyediting, typesetting, and review of the resulting proof before it is published in its final citable form. Please note that during the production process errors may be discovered which could affect the content, and all legal disclaimers that apply to the journal pertain.

newly identified pathway may be relevant to the microbiota-gut-brain axis and immune homeostasis in humans.



INTRODUCTION

Innate host defenses, including antimicrobial peptides from the intestinal epithelium, are essential for defense against infection and for maintenance of the healthy microbiota (Hooper, 2015; Peterson and Artis, 2014). Although much is known about innate defenses in myeloid and lymphoid cells, much less is known about the regulation of antimicrobial peptide expression in the intestinal epithelium. Nonetheless, the intestinal epithelium is the most conserved host defense system (Bosch et al., 2009).

Caenorhabditis elegans gene *clec-60* encodes a secreted C-type lectin related to mammalian antimicrobial lectin RegIII γ (Vaishnav et al., 2011). *clec-60* is upregulated in the intestinal epithelium during infection with Gram-positive pathogens, such as *Enterococcus faecalis*, *Microbacterium nematophilum*, and *Staphylococcus aureus* (O'rourke et al., 2006; Wong et al., 2007; Irazoqui et al., 2010), as well as Gram-negative *Yersinia pestis* (Bolz et al., 2010). In contrast, *clec-60* is repressed by *Pseudomonas aeruginosa* and *Salmonella enterica* (Irazoqui et al., 2010; Head and Aballay, 2014). Overexpression of *clec-60* results in enhanced host survival of infection (Irazoqui et al., 2010). Although differential expression of *clec-60* suggests that it is controlled by pathogen-specific signal transduction pathways, the identity of such pathways is unknown. Thus, the dynamic and pathogen-specific expression profile of *clec-60* makes an attractive model to investigate pathways that control the host response to infection.

Mammals and most invertebrates share a dependence on Toll-Like Receptors (TLRs) in the detection of Gram-positive bacterial infection (Akira et al., 2006). However, nematodes lack important components of canonical TLR pathways (Pujol et al., 2001). They also lack Nacht and Leucine-Rich domain containing proteins (NLRs). Despite the absence of both pattern

recognition receptor (PRR) pathways, nematodes mount pathogen-specific transcriptional host responses to *S. aureus* (Irazoqui et al., 2010; Wong et al., 2007). Therefore, nematodes must possess a mechanism to detect *S. aureus* infection. In mammals, N-formyl peptides produced by bacteria are triggers of innate immune responses through the G-protein-coupled receptors (GPCRs), formyl peptide receptors 1 and 2 (Bloes et al., 2015). In *C. elegans*, the GPCR superfamily is greatly expanded (Rubin et al., 2000). GPCRs NPR-1 and FSHR-1 are involved in the *C. elegans* transcriptional and behavioral response to Gram-negative *P. aeruginosa* (Aballay et al., 2008; Powell et al., 2009). Because of this precedent, we hypothesized that a GPCR might function in the detection of *S. aureus*.

Instead, our studies revealed an unexpected connection between the canonical Wnt pathway and the neurotransmitter acetylcholine (ACh). Canonical Wnt signaling is important for intestinal development, homeostasis, and carcinogenesis in humans (Clevers and Nusse, 2012). In addition, it plays important roles in the function and activation of cells of the immune system (Silva-García et al., 2014). Disentangling the direct involvement of the canonical pathway in innate immunity from indirect roles through cellular differentiation remains challenging in mammalian models. In contrast to mammals, the nematode intestinal epithelium comprises just 20 fully differentiated cells (McGhee, 2007). These cells do not undergo anoikis, but remain functional for the entire life of the animal. Thus, canonical Wnt signaling in *C. elegans* is not involved in epithelial tissue renewal as it is in mammals, which greatly facilitates the study of its role in antimicrobial peptide production.

ACh secreted by cholinergic neurons engages ACh receptors on postsynaptic cells, including neurons and muscle cells. ACh receptors can be either muscarinic or nicotinic, which are GPCRs and ligand-gated ion channels, respectively (Rand, 2007). Muscarinic receptors engage downstream signaling pathways involving G_q, G₁₁, G_i, or G₀ heterotrimeric G proteins, depending on muscarinic receptor and cell type, to produce changes in gene expression and cellular function (Wess et al., 2007). In the central nervous system, muscarinic signaling is important for several behavioral and sensory processes, and has been implicated in Alzheimer's disease and Parkinson's disease. Peripheral muscarinic signaling controls cardiac rhythm, smooth-muscle contraction, and glandular secretion (Wess et al., 2007). In this work, we expanded the known roles of the muscarinic pathway to that of controlling host defense gene expression in the intestinal epithelium via the Wnt pathway. Because direct epithelial-neuronal synapses have not been described in this or any other organism (White et al., 1986; Yoo and Mazmanian, 2017), in *C. elegans* infection ACh appears to function in an endocrine fashion to engage muscarinic receptors in the intestinal epithelium and induce the expression of host defense genes through the activation of Wnt pathway.

RESULTS

Muscarinic signaling controls host defense

In addition to infection, induction of *clec-60* was reported under conditions of nutritional deprivation (Melo and Ruvkun, 2012). To compare the induction of *clec-60* under both conditions, we examined the expression of transcriptional reporter *clec-60p::gfp* (Irazoqui et al., 2008). In control animals fed *ad libitum* with *Escherichia coli* strain OP50, the standard

laboratory diet, GFP expression was minimal (Fig. 1A). We observed similarly low GFP expression in animals that were starved for 8 h on the medium used in *S. aureus* infection assays (Fig. 1A, B). In contrast, animals that had been infected by feeding with *S. aureus* for 8 h exhibited greatly enhanced GFP expression in the intestinal epithelium (Fig. 1A, B). Thus, nutritional deprivation did not induce *clec-60p::gfp* under conditions used in *S. aureus* infection assays.

To identify GPCRs involved in pathogen detection upstream of *clec-60*, we performed a screen, in which we examined the induction of *clec-60p::gfp* by *S. aureus* in animals that had been treated with individual RNAi against 890 GPCR genes. Silencing of *gar-2* resulted in defective GFP expression (Fig. S1A). Mutants defective in *gar-2* function lived slightly longer than wild type on nonpathogenic *E. coli* (Fig. S1B) but exhibited a mild defect in survival of infection (Fig. S1C), suggesting that their response defect was biologically important. *gar-2* encodes a muscarinic receptor (Hobert, 2013). The *C. elegans* genome contains two other genes for muscarinic receptors (*gar-1* and *gar-3*), raising the possibility of redundancy. Simultaneous silencing of *gar-2* and *gar-3* synergistically reduced *clec-60p::gfp* induction (Fig. 1C, D), suggesting that *gar-2* and *gar-3* share redundant functions.

To determine if the activation of muscarinic receptors can elicit a similar response, we used the ACh-mimic arecoline (Gilani et al., 2004). Administration of arecoline to uninfected (*i.e.* *E. coli*-fed) animals was sufficient to induce *clec-60p::gfp* expression similar to that in infected animals (Fig. 1C, E). Arecoline also induced the endogenous expression of host defense genes *clec-60*, *ilys-3*, and *lys-5* (Irazaqui et al., 2010). Furthermore, silencing of *gar-2* and *gar-3* abrogated arecoline-induced *clec-60* expression (Fig. 1C, E). Muscarinic antagonist scopolamine (Hwang et al., 1999) impaired *clec-60p::gfp* induction by either *S. aureus* or arecoline (Fig. 1G–I). Oxotremorine, a specific muscarinic agonist, also induced *clec-60* (Fig. 1J). Collectively, these results showed that muscarinic activation is necessary and sufficient for the induction of the host response to *S. aureus*.

Treatment with arecoline 24 h prior to infection led to significantly enhanced survival of infection (Fig. 1K) with no effect on aging (Fig. 1L). In contrast, scopolamine enhanced susceptibility to *S. aureus* (Fig. 1M). However, scopolamine also caused reduced lifespan on nonpathogenic *E. coli* (Fig. 1N). Mutants defective in gene *unc-17*, which encodes the vesicular ACh transporter (vAChT) necessary for loading ACh in synaptic vesicles (Alfonso et al., 1993), have impaired ACh release. *unc-17*(vAChT) mutants were significantly susceptible to infection (Fig. 1O) with a minor aging defect (Fig. S1D). Aldicarb is a cholinesterase inhibitor that prevents the hydrolysis of ACh in neuromuscular junctions, resulting in paralysis. Aldicarb paralysis assays are useful for estimating the endogenous concentration of ACh in *C. elegans* (Mahoney et al., 2006). We used aldicarb paralysis assays to estimate the endogenous amount of ACh in animals that were infected with *S. aureus* for 20 min. Infected animals paralyzed 30% faster than control animals fed *E. coli* (Fig. 1P), indicating that endogenous ACh is released during infection.

Taken together, these observations supported a hypothesis that *S. aureus*, and cholinergic agonists oxotremorine and arecoline, trigger muscarinic receptors GAR-2 and GAR-3, resulting in the induction of downstream host defense genes (Fig. 1Q).

Gαq, phospholipase Cβ, and protein kinase Cη function downstream of muscarinic receptors to promote host defense

The muscarinic receptor pathway has been delineated partially in *C. elegans*. Muscarinic receptor GAR-3 signals through the α subunit of heterotrimeric G protein q (Gαq, encoded by gene *egl-30*), which activates phospholipase Cβ (PLCβ, encoded by *egl-8*) (Lackner et al., 1999; Miller et al., 1999; Steger and Avery, 2004). Silencing of either *egl-30* or *egl-8* abrogated *clec-60p::gfp* induction by infection (Fig. 2A, B) and mutants lacking *egl-8* were unable to induce *clec-60* (Fig. 2C). RNAi of *egl-30* or *egl-8* also prevented *clec-60p::gfp* induction by arecoline (Fig. 2D, E). Taken together, these results suggested that ACh may signal through a pathway controlled by GAR-2 and -3, which includes EGL-30 (Gαq) and EGL-8 (PLCβ). In support of this idea, we recently showed that EGL-30 is important during host defense (Najibi et al., 2016). In addition, we found that *egl-8* mutants were unable to induce *clec-60* in response to arecoline (Fig. 2F) and that, while the longevity of *egl-8* mutants was slightly extended (Fig. 2H), their survival of infection was severely compromised (Fig. 2G). These results indicated that the EGL-30-EGL-8 axis plays an important and specific role for host defense against *S. aureus* downstream of ACh.

PLCβ is a major signaling hub (Rebecchi and Pentylala, 2000). It catalyzes the hydrolysis of phosphatidylinositol 4,5-bisphosphate (PIP₂) to generate diacyl glycerol (DAG) and inositol trisphosphate (IP₃), second messengers that control a plethora of downstream signaling pathways. To identify signaling components that may function downstream of EGL-8 (PLCβ) during infection, we performed a screen to identify RNAi clones from a kinome library that prevented *clec-60p::gfp* induction by *S. aureus*. This screen identified *pkc-1* (Fig. 2A, B), which encodes protein kinase Cη (PKCη) that is activated by diacyl glycerol (Stahelin et al., 2004). *pkc-1* RNAi also abrogated the induction of *clec-60p::gfp* by arecoline (Fig. 2D, E). Partial loss-of-function *pkc-1* mutants exhibited mildly defective host survival of infection (Fig. 2I), while their aging phenotype was unaffected (Fig. 2J). Whether such mild phenotype was a consequence of incomplete expressivity of the allele, or of partial redundancy with additional protein kinases, is unclear. Nonetheless, these results suggested that PKC-1 (PKCη) is an important signaling component of the pathway that links muscarinic receptors with host defense gene induction (Fig. 2K).

Wnt ligand is induced in response to infection and to acetylcholine

clec-60 induction by *S. aureus* is dependent on the β-catenin homolog *bar-1*, which functions within the canonical Wnt pathway (Irazoqui et al., 2008). To examine the role of the canonical Wnt pathway, we measured expression of key components during infection. Genes *cwn-2*, which encodes a Wnt ligand, and *mig-1*, which encodes Wnt receptor Frizzled, were highly induced, while Wnt gene *mom-2* and Frizzled gene *mom-5* were repressed (Fig. 3A). Furthermore, we found marked infection-induced expression of a translational reporter for CWN-2, in the intestinal epithelium (Fig. 3B, C). A transcriptional reporter for *mig-1* was similarly induced (Fig. 3D, E). Thus, Wnt and its receptor were induced by *S. aureus* in the tissue where infection took place.

Systemic administration of arecoline or oxotremorine was sufficient to induce *cwn-2* expression in uninfected animals (Fig. 3F, G). The CWN-2 reporter showed specific

induction in the intestinal epithelium (Fig. 3H, I), as with infection. *unc-17* mutants were unable to induce *cwn-2* and *clec-60* during infection (Fig. 3J, Fig. S1E), demonstrating that endogenous ACh was necessary. Furthermore, silencing of *gar-2* and *-3*, *egl-30*, *egl-8*, and *pkc-1*, prevented induction of the CWN-2 translational reporter by infection (Fig. 3K). *egl-8* mutation abrogated *cwn-2* induction by arecoline in uninfected animals (Fig. 3L). These results showed that Wnt ligand was induced in the intestinal epithelium by the muscarinic pathway, and that muscarinic activation was both necessary and sufficient for epithelial induction of *cwn-2*.

Aldicarb assays showed that endogenous ACh amounts rose very quickly during infection, peaking at 10 min, and then diminishing and plateauing after 4 h (Fig. 3M). In contrast, endogenous *cwn-2* and *clec-60* mRNA concentrations showed highest expression after 16 h of infection (Fig. 3N). Together, these data supported a hypothesis that *S. aureus* induced ACh release, which drove the muscarinic pathway, whose activation induced Wnt ligand and Frizzled receptor in the intestinal epithelium (Fig. 3O).

Canonical Wnt signaling is necessary and sufficient for defense gene induction

Silencing of positive regulators in the canonical Wnt pathway (Sawa and Korswagen, 2013), including homologs of Wnt, Frizzled, Disheveled, β -catenin, and TCF(LEF), abrogated induction of *clec-60p::gfp* by *S. aureus* (Fig. 4A, B). Silencing of Frizzled homolog *mig-1* impaired induction of a set of host response genes (Fig. 4C). Additionally, silencing of the Wnt signaling genes impaired induction of *clec-60p::gfp* by arecoline (Fig. 4D, E). Silencing of negative regulators in the canonical Wnt pathway, including homologs of Axin, Casein kinase I, and β -TrCP, resulted in constitutive induction of *clec-60p::gfp* in uninfected animals (Fig. 4F, G) in a *bar-1* (β -catenin)-dependent manner (Fig. 4G). Silencing of negative regulator gene *gsk-3*, homologous to mammalian glycogen synthase kinase 3 β (GSK-3 β), resulted in constitutively high expression of several host defense genes in uninfected animals (Fig. 4H). Taken together, these results showed that activation of the canonical Wnt signaling pathway was necessary and sufficient to induce host defense gene expression by infection and by ACh.

Mutants defective in *cwn-2* or *mig-1* exhibited impaired infection survival (Fig. 4I, K) with no effect on aging (Fig. 4J, L). *gsk-3* silencing resulted in enhanced host survival (Fig. 4M), even when it negatively affected aging (Fig. 4N). In contrast, *gsk-3* silencing had no effect in animals lacking *bar-1* function (Fig. 4O). These results demonstrated how activation of the canonical Wnt pathway enhanced host defense in a *bar-1* (β -catenin)-dependent manner.

Arecoline administration, which activates muscarinic signaling, also resulted in enhanced survival of infection, while administration of scopolamine, which inhibited muscarinic signaling, impaired survival (Fig. 4P). Deletion of *mig-1* (Frizzled) abrogated such effects (Fig. 4Q), again placing the Wnt pathway genetically downstream of muscarinic signaling. Muscarinic and Wnt pathway mutants showed no defects in aldicarb paralysis assays, ruling out the possibility that such mutations decrease ACh release (Fig. S2C to H). RNAi of *egl-8* (PLC β) or double RNAi of *gar-2* and *gar-3* did not enhance susceptibility in *bar-1* (β -catenin) mutants, suggesting by epistasis analysis that *gar-2*, *gar-3*, *egl-8* (PLC β), and *bar-1* (β -catenin) functioned in the same pathway (Fig. S2A). Additionally, *unc-17*, *egl-8*, and

bar-1 null mutants showed similar susceptibilities to infection (Fig. S2B). Collectively, these observations supported a genetic pathway (Fig. 4R) in which *S. aureus* stimulated the release of ACh, which activated the muscarinic pathway, driving transcription of *cwn-2* and *mig-1* in the intestinal epithelium. Such activation of Wnt engaged the canonical Wnt pathway, resulting in the transcription of downstream host defense genes.

Canonical Wnt signaling functions post-developmentally

A key prediction of the pathway proposed in Fig. 4R is that the canonical Wnt pathway is activated in adult animals during infection, after its known roles in development (Sawa and Korswagen, 2013). The induction of *cwn-2* and *mig-1* in the intestinal epithelium strongly supports this prediction. Post-embryonic RNAi-mediated silencing has been used to circumvent developmental effects of key conserved genes, revealing phenotypes that would otherwise be masked by developmental defects or inviability (Curran, 2007). Adult-specific silencing of *cwn-2*, *mig-1*, and *bar-1* resulted in defective host survival of infection (Fig. 5A, C, E), with little to no effect on aging (Fig. 5B, D, F), suggesting that the Wnt pathway functions during adulthood for host defense. Inorganic lithium compounds are known GSK-3 β chemical inhibitors in clinical use. Brief administration of LiCl to adult uninfected animals resulted in high induction of *clec-60p::gfp* in a *bar-1*-dependent manner (Fig. 5G, H). Together, these results showed that post-developmental activation of canonical Wnt signaling in adult animals was necessary and sufficient for induction of host defense genes in the intestinal epithelium.

Muscarinic and Wnt signaling take place in the intestinal epithelium

Because intestinal epithelial *clec-60* induction is under control of the canonical Wnt pathway, we examined whether the Wnt pathway functions in the intestinal epithelium. We adopted a method to produce RNAi-mediated silencing specifically in the intestinal epithelium (Luallen et al., 2015; Qadota et al., 2007). Intestine-specific silencing of genes *mig-1* or *bar-1* greatly impaired host survival of infection (Fig. 6A, B) with minor detrimental effects on aging. As mentioned, *cwn-2* mutants exhibited defective survival of infection (Fig. 4I), but not defective aging (Fig. 4J). Re-expression of wild type *cwn-2* only in the intestinal epithelium partially restored survival of infection in these mutants (Fig. 6D), whereas muscle-specific expression did not (Fig. 6E). Similarly, intestinal expression of *mig-1* restored survival of infection in *mig-1* mutants almost completely (Fig. 6F). These results showed that the canonical Wnt pathway functioned in the intestinal epithelium for host defense.

Because both *unc-17* (the vesicular ACh transporter) and *cha-1* (choline acetyltransferase) are expressed exclusively in the nervous system of *C. elegans*, it is thought that ACh is produced and released only by neurons in nematodes (Alfonso et al., 1993; Duerr et al., 2008; Pereira et al., 2015). We wondered if the muscarinic pathway might also function in the intestinal epithelium. Intestinal silencing of *gar-2* or *gar-3* caused mild infection survival defects (Fig. S3A, B), whereas simultaneous *gar-2* and *gar-3* silencing caused a strong defect (Fig. 6G), suggesting that these two receptors share redundant functions in the intestine. Simultaneous *gar-2*, *gar-3* intestinal silencing greatly extended the lifespan of non-infected animals (Fig. 1I), ruling out that the enhanced susceptibility to infection was due to a defect

in viability or aging. In addition, colony forming unit (cfu) assays did not show a difference in bacterial load between treated and control animals, indicating that the enhanced susceptibility was not caused by enhanced bacterial colonization of, or residence in, the intestine (Fig. S3C). Intestinal RNAi of *egl-30* (Gαq) or of *egl-8* (PLCβ) also strongly impaired host survival (Fig. 6G), but resulted in minor reductions of lifespan on *E. coli*, suggesting a possible role in aging (Fig. 6H). These results showed that the muscarinic pathway performed important functions for host defense in the intestinal epithelium.

Identification of transcription factors that link muscarinic and Wnt signaling

The results so far indicated that the muscarinic pathway and the downstream Wnt pathway functioned in the intestinal epithelium to control host defense gene induction. However, the mechanism of the connection between these two pathways was unknown. We determined that muscarinic signaling caused induction of *cwn-2* (Fig. 3F–L), implying the existence of transcription factors that mediate muscarinic-induced Wnt induction. Therefore, we performed a reverse genetic screen to identify such transcription factors. Following gene silencing, we administered arecoline and measured *clec-60p::gfp*. Thus, we identified 10 transcription factor genes that were required for full *clec-60p::gfp* induction by arecoline (Fig. 7A). Because these transcription factors could be involved upstream or downstream of Wnt signaling, we measured *cwn-2* induction after arecoline treatment. We expected genes that function as a link between muscarinic and Wnt signaling to disrupt *cwn-2* induction by arecoline. Out of the 10 candidate genes, only 4 satisfied this criterion (Fig. 7B). Because of the availability of genetic tools and its evolutionary conservation, we decided to focus on one such gene, *lin-1*, which is homologous to human *ELK1-3* transcription factor genes with known roles in inflammation (Oettgen, 2006).

Genetic deletion of *lin-1* (*ELK*) partially impaired arecoline induction of *clec-60* (Fig. 7C) and strongly impaired induction of *cwn-2* (Fig. 7D). A gain of function allele of *lin-1* (*ELK*) was sufficient for high constitutive expression of *clec-60* (Fig. 7E) and *cwn-2* (Fig. 7F) in uninfected animals. These results indicated that *lin-1* was sufficient and partially necessary for host defense gene induction downstream of ACh.

Intestine-specific silencing of *lin-1* (*ELK*) strongly impaired host survival of infection (Fig. 7G), with no effect on aging (Fig. 7H). Furthermore, genetic epistasis experiments showed a lack of effect of *lin-1* RNAi in the survival of infected *bar-1* (β-catenin) mutants (Fig. S5), consistent with *lin-1* (*ELK*) and *bar-1* (β-catenin) participating in the same pathway. Thus, *lin-1* (*ELK*), and potentially other genes identified in our screen, mediate control of Wnt signaling by the muscarinic pathway.

DISCUSSION

C. elegans possess a simple nervous system, comprising 302 neurons (White et al., 1986). *C. elegans* neurons are divided into sensory, interneuron, and motor neuron classes. A majority of the neurons in *C. elegans* serve sensory functions and are present in the anterior head region, where they are organized into ganglia surrounding the pharynx. About 150 neurons are thought to synthesize and release ACh (Duerr et al., 2008; Pereira et al., 2015).

Sensory, interneuron, and motor neurons can be cholinergic. Synapses connecting neurons and the intestinal epithelium have not been observed.

Our results suggested that ACh, released from the nervous system in response to infection with *S. aureus*, functioned in a neuroendocrine fashion to activate muscarinic receptors in the intestinal epithelium. This activation led to increased expression of Wnt and its receptor Frizzled in the intestinal epithelium. Wnt, presumably secreted to the basolateral side of the polarized epithelium, could signal to the intestinal epithelial cells in an autocrine and paracrine fashion. Activation of the canonical Wnt pathway led to the induction of host defense genes, including antimicrobials such as C-type lectin *cllec-60* and lysozymes. The genetic link between the muscarinic and Wnt pathways was mediated by at least four highly conserved transcription factors, including the Ets family transcription factor LIN-1, which is homologous to human transcription factors ELK1-3.

The nervous system may have evolved to stimulate cells distal from the site of activation, injury, or infection to help produce an integrated physiological response to insult. Also, this mechanism may allow the translation of a fast and short-lived signal (ACh) to a slow and longer-lived signal (Wnt ligand) to produce a robust response to infection. Furthermore, release of ACh increases *C. elegans* locomotion (Rand, 2007). Pathogen-triggered ACh release may thus provide an elegant way of coupling emergency evasive behaviors with the enhanced expression of host defense genes. This view is supported by previous work, which showed that cholinergic signaling is involved in the behavioral response to infection by *Microbacterium nematophilum* (McMullan et al., 2012).

Our studies highlight muscarinic signaling as a key mechanism by which the nervous system controls intestinal epithelial host defense. In mice and humans, the vagal nerve and the enteric nervous system project cholinergic fibers to the viscera and the intestinal epithelium (Erickson et al., 2014; Foong et al., 2014; Gautron et al., 2013; Jönsson et al., 2007; Matteoli and Boeckxstaens, 2013). Muscarinic receptors are broadly expressed in the mammalian intestinal epithelium (Harrington et al., 2010; Khan et al., 2013). *In vitro*, muscarinic stimulation of intestinal epithelial cells modulated ion secretion, cell proliferation, and barrier permeability and repair (Hirota and McKay, 2006; Khan et al., 2014; Peng et al., 2013). However, mammalian epithelial cells and other cells are capable of producing and secreting non-neuronal ACh (Grando et al., 2015). Therefore, muscarinic signaling at the mammalian intestinal epithelium is complex and its function is poorly understood.

Nonetheless, emerging clues hint that epithelial muscarinic signaling is important for immune homeostasis at several mucosal sites in mammals. For example, muscarinic stimulation of intestinal epithelial cells prevents barrier disruption under inflammatory conditions (Dhawan et al., 2015). *OCTNI*, which encodes an ACh exporter, is a susceptibility locus for Crohn's disease (Pochini et al., 2012). Muscarinic stimulation causes IL-8 secretion by bronchial epithelial cells, driving inflammation (Profita et al., 2008). Muscarinic signaling is important during experimental sepsis (Amaral et al., 2016; Jeremias et al., 2016), and anticholinergic treatment is associated with community-acquired pneumonia in elderly adults (Chatterjee et al., 2016). Mice lacking M3 muscarinic receptor exhibit impaired pro-inflammatory signaling and clearance of bacterial and helminth

infections (Darby et al., 2015; McLean et al., 2015). Secretion of ACh by mouse T cells enhances antimicrobial peptide production by the intestinal epithelium via muscarinic signaling (Dhawan et al., 2016). Anti-muscarinic therapies for the treatment of inflammation are being considered in diseases such as chronic obstructive pulmonary disease (COPD) or inflammatory bowel disease (IBD) (Matera et al., 2014; Sales, 2010; Verbout and Jacoby, 2012). However, the molecular mechanisms by which muscarinic signaling enhances mucosal host defense are not known.

The canonical Wnt pathway plays several important roles in the mammalian intestinal epithelium, including development, homeostasis, and repair after inflammation (Karin and Clevers, 2016). Wnt signaling within Paneth cells (crypt epithelial cells specialized for antimicrobial peptide secretion) is critical for antimicrobial gene expression (Clevers and Bevins, 2013; Clevers et al., 2007). Wnt signaling defects in Paneth cells are associated with IBD (Bevins and Salzman, 2011; Clevers et al., 2007; Kini et al., 2015; Koslowski et al., 2009, 2012). Thus, our delineation of a canonical Wnt pathway that is important for antimicrobial peptide expression in the nematode intestine highlights evolutionary conservation of its host defense function.

We identified four conserved transcription factor genes as genetic links between the muscarinic and Wnt pathways. *hlh-26* has weak resemblance to human genes *HEYL* and *ARNTL2*, and *hlh-34* is related to *NPAS3* and *HIF1A*. *ceh-6* and *lin-1* are homologous to human genes *POU3F1-4* and *ELK1-3*, respectively. *lin-1* is under control of the ERK signaling cascade in *C. elegans* (Lackner and Kim, 1998), and had not been implicated in host defense previously. Human ELK1 is activated downstream of muscarinic-Gαq-PKC signaling (Blaukat et al., 2000; Rössler et al., 2008). Both ELK1 and ELK3 are known to be important for host defense induced by bacterial peptidoglycan and for phagocytosis of bacteria by macrophages (Tsoyi et al., 2015; Xu et al., 2001). Thus, our results placing *lin-1* (*ELK*) as a link between upstream muscarinic signaling and downstream Wnt signaling are of great importance.

Genetic and pharmacological inhibition of muscarinic signaling reduces intestinal epithelial cell proliferation and carcinogenesis in mice (Raufman et al., 2008). In humans, cholinergic fibers of the vagal nerve enhance gastric tumorigenesis, by enhanced Wnt3 expression driven by the M3 muscarinic receptor (Zhao et al., 2014). This observation provides a striking clinical parallel to our results, highlights their clinical relevance, and suggests that the implications of our findings may transcend host-pathogen interactions. Moreover, members of the human microbiota are able to produce physiologically relevant quantities of ACh (Sarkar et al., 2016), perhaps providing a direct mechanism of microbiota-epithelium interaction, and an avenue of therapeutic intervention for chronic inflammation. It seems likely that cholinergic induction of Wnt in the gut epithelium constitutes a fundamental mechanism of the so-called Gut-Brain-Microbiota axis of immune homeostasis (Dhawan et al., 2012; Tracey, 2014).

STAR★Methods

Contact for Reagents and Resources

Further information and requests for reagents may be directed to, and will be fulfilled by the corresponding author Javier E. Irazoqui (Javier.Irazoqui@umassmed.edu).

Experimental Model

***C. elegans* strains**—*C. elegans* strains were grown on nematode-growth media (NGM) plates seeded with *E. coli* OP50 at 15 – 20 °C, according to standard procedures (Powell and Ausubel, 2008).

Method Details

Infection—*S. aureus* HA-MRSA USA100 (Carroll et al., 2013) was grown overnight in tryptic soy broth (TSB) containing 50 µg/ml kanamycin (KAN). 10 µl of overnight cultures was uniformly spread on the entire surface of 35 mm TSA plates containing 10 µg/ml kanamycin, and incubated 4–6 h at 37 °C. Animals were treated with 80–100 µg/ml 5-fluoro-2'-deoxyuridine (FU DR) at L4 larval stage for 24 h at 15 °C before transfer to *S. aureus* plates. After FU DR treatment, 25 – 40 infertile animals were transferred to each of three replicate infection plates per strain. Survival was quantified as described (Powell and Ausubel, 2008). Animals that died of bursting vulva, matricidal hatching, or crawling off the agar were censored.

Starvation—Worms were supplemented with 80–100 µg/ml FU DR at L4 larval stage for 24 h at 15 °C before transfer to solid TSA plates without bacteria. After 8 h, animals were harvested for imaging.

Longevity (aging) assays—All assays were performed as described in (Powell and Ausubel, 2008). Animals were transferred to NGM plates seeded with *E. coli* OP50, supplemented with 80 – 100 µg/ml FU DR and incubated at 25 °C. Experiments were performed at least twice.

RNAi by feeding—RNAi was carried out using bacterial feeding RNAi (Timmons et al., 2001). Briefly, 8 to 12 gravid adult worms were spot-bleached in 20% alkaline hypochlorite solution directly on the plates (outside the bacterial lawn) to synchronize progeny. Progeny of bleached adults were treated with FU DR at the L4 larval stage for 24 h at 15 °C prior to use. The RNAi plates contain *E. coli* HT115 carrying vector L4440 (empty vector) or expressing dsRNA of selected genes. Adult RNAi treatment was done by incubating young adult animals for 2 days at 15 °C on RNAi plates. *gar-2* and *gar-3* double RNAi plates were prepared by adding a mixture of 150 µl of overnight culture of HT115 carrying *gar-2* RNAi and 150 µl of HT115 carrying *gar-3* RNAi. HT115 RNAi clones were obtained from the Ahringer genomic RNAi library, or the Vidal library when absent in the former. Clone identity was confirmed by sequencing, and absence of off target effects was verified against predictions by the *C. elegans* genomic database resource, WormBase (www.wormbase.org). RNAi gene silencing was confirmed by real-time RT-PCR (Fig. S4).

RNAi Screening—Briefly, 2,000 gravid adult, *clec-60p::gfp* worms were bleached with alkaline hypochlorite, followed by several washes with M9 buffer (Powell and Ausubel, 2008). Subsequently, the eggs were incubated in M9 buffer overnight at room temperature. RNAi was carried out using bacterial feeding on L1 stage animals in a semi-automated liquid setup until they reached the young adult stage at 15 °C (Lehner et al., 2006). Following RNAi treatment, animals were washed and transferred to solid medium in 96 well plates containing *S. aureus* for the induction of *clec-60p::gfp*. The RNAi sub-libraries used, assembled from the Ahringer and Vidal genomic libraries, were: GPCRs (1748 genes; assembled by Justine Melo, MGH), protein kinases (441 genes; assembled by Javier Irazoqui, MGH), and transcription factors (427 genes; assembled by Sean Curran and Dave Simon, MGH).

Aldicarb assays—Aldicarb paralysis after infection was performed using a previously described protocol (Mahoney et al., 2006) with minor changes. Briefly, 30 young adult animals were placed for 10 min to 12 h on infection plates. Next, animals were immediately transferred to TSA (Tryptic Soy Agar) plates containing 1 mM aldicarb (Sigma-Aldrich) and 100 µl of 10X overnight culture of OP50. Paralysis was quantified blindly at room temperature.

qRT-PCR—After treatment, *C. elegans* were collected in M9 buffer and lysed using TRI Reagent (Molecular Research Center) following manufacturer's instructions. cDNA was obtained with iScript cDNA (Bio-Rad) and qRT-PCR was performed using iQ SYBR Green (Bio-Rad), as described previously (Irazoqui et al., 2010). Data analysis was performed using the Pfaffl method (Pfaffl, 2001).

Imaging—Animals expressing a fluorescent reporter gene were kept for 1 h at room temperature prior to imaging. Animals were next harvested by washing with M9 buffer (Powell and Ausubel, 2008), and paralyzed with 10 % NaN₃ in half-well 96-well plates. Image acquisition was automatically performed using a Cytation 3 Imaging Plate Reader (Biotek).

Drug treatments—Arecoline hydrobromide (Sigma, 31593-250MG), 1 mM for killing assays and 5 mM for other experiments; Scopolamine (Sigma PHR1470-500MG), 1 mM for killing assays and 5 mM for other assays; Oxotremorine (sigma, O100-100MG) 1 mM, LiCl (Sigma 203637-10G) 100 mM). For killing assays and qRT-PCR, all drug treatments were performed on solid NGM plates supplemented with drug. Animals were treated at the young adult stage and incubated at 25 °C for 24 h. After 16 h, animals were harvested for killing assays or qRT-PCR. For reporter gene quantification, all drug treatments were performed in NGM liquid culture for 16 h. Subsequently, animals were washed with M9 buffer and prepared for imaging.

Quantification and Statistical Analysis

Statistical analyses were performed using Prism 6 software (GraphPad). Survival data were compared using the Log-Rank test. Data are represented as median survival (MS), as defined by Kaplan-Meier analysis, or Time to 50% Death (LT₅₀), as defined by nonlinear regression.

A p value < 0.05 was considered significantly different from control. For qRT-PCR, two-sample, two-tailed t tests were performed to evaluate differences among pooled Ct values according to Pfaffl (Pfaffl, 2001) using Excel. A p value < 0.05 was considered significant. For image quantification, two-sample, two-tailed t tests were performed. Prior to use of the t -test, all values were confirmed for normal distribution by the Agostino Pearson omnibus test.

Supplementary Material

Refer to Web version on PubMed Central for supplementary material.

Acknowledgments

Dr. Frederick Ausubel and his laboratory provided generous intellectual input and shared laboratory space and equipment. Research reported in this publication was supported by the National Institute of General Medical Sciences of the National Institutes of Health under award number GM101056, and by the National Science Foundation under award number NSF1457055 (to J.E.I.). Some strains were provided by the CGC, which is funded by the NIH Office of Research Infrastructure Programs (P40 OD010440). The content is solely the responsibility of the authors and does not necessarily represent the official views of the National Institutes of Health.

References

- Aballay A, Styer KL, Singh V, Macosko E, Steele SE, Bargmann CI. Innate immunity in *Caenorhabditis elegans* is regulated by neurons expressing NPR-1/GPCR. *Sci N Y NY*. 2008; 322:460–464.
- Akira S, Uematsu S, Takeuchi O. Pathogen recognition and innate immunity. *Cell*. 2006; 124:783–801. [PubMed: 16497588]
- Alfonso A, Grundahl K, Duerr J, Han H, Rand J. The *Caenorhabditis elegans* unc-17 gene: a putative vesicular acetylcholine transporter. *Sci N Y NY*. 1993; 261:617–619.
- Amaral FA, Fagundes CT, Miranda AS, Costa VV, Resende L, Gloria de Souza D, da Prado VF, Teixeira MM, Maximo Prado MA, Teixeira AL. Endogenous Acetylcholine Controls the Severity of Polymicrobial Sepsis-associated Inflammatory Response in Mice. *Curr Neurovasc Res*. 2016; 13:4–9. [PubMed: 26500102]
- Bevins CL, Salzman NH. Paneth cells, antimicrobial peptides and maintenance of intestinal homeostasis. *Nat Rev Microbiol*. 2011; 9:356–368. [PubMed: 21423246]
- Blukat A, Barac A, Cross MJ, Offermanns S, Dikic I. G Protein-Coupled Receptor-Mediated Mitogen-Activated Protein Kinase Activation through Cooperation of G α_q and G α_i Signals. *Mol Cell Biol*. 2000; 20:6837–6848. [PubMed: 10958680]
- Bloes DA, Kretschmer D, Peschel A. Enemy attraction: bacterial agonists for leukocyte chemotaxis receptors. *Nat Rev Microbiol*. 2015; 13:95–104. [PubMed: 25534805]
- Bolz DD, Tenor JL, Aballay A. A conserved PMK-1/p38 MAPK is required in *caenorhabditis elegans* tissue-specific immune response to *Yersinia pestis* infection. *J Biol Chem*. 2010; 285:10832–10840. [PubMed: 20133945]
- Bosch TCG, Augustin R, Anton-Erxleben F, Fraune S, Hemmrich G, Zill H, Rosenstiel P, Jacobs G, Schreiber S, Leippe M, et al. Uncovering the evolutionary history of innate immunity: the simple metazoan *Hydra* uses epithelial cells for host defence. *Dev Comp Immunol*. 2009; 33:559–569. [PubMed: 19013190]
- Carroll RK, Burda WN, Roberts JC, Peak KK, Cannons AC, Shaw LN. Draft Genome Sequence of Strain CBD-635, a Methicillin-Resistant *Staphylococcus aureus* USA100 Isolate. *Genome Announc*. 2013:1.
- Chatterjee S, Carnahan RM, Chen H, Holmes HM, Johnson ML, Aparasu RR. Anticholinergic Medication Use and Risk of Pneumonia in Elderly Adults: A Nested Case-Control Study. *J Am Geriatr Soc*. 2016; 64:394–400. [PubMed: 26889844]

- Clevers HC, Bevins CL. Paneth cells: maestros of the small intestinal crypts. *Annu Rev Physiol*. 2013; 75:289–311. [PubMed: 23398152]
- Clevers HC, Nusse R. Wnt/ β -Catenin Signaling and Disease. *Cell*. 2012; 149:1192–1205. [PubMed: 22682243]
- Clevers HC, Wehkamp J, Wang G, Kübler I, Nuding S, Gregorieff A, Schnabel A, Kays RJ, Fellermann K, Burk O, et al. The Paneth cell alpha-defensin deficiency of ileal Crohn's disease is linked to Wnt/Tcf-4. *J Immunol Baltim Md 1950*. 2007; 179:3109–3118.
- Curran SP. Lifespan regulation by evolutionarily conserved genes essential for viability. *PLoS Genet*. 2007; 3:e56. [PubMed: 17411345]
- Darby M, Schnoeller C, Vira A, Culley F, Bobat S, Logan E, Kirstein F, Wess J, Cunningham AF, Brombacher F, et al. The M3 Muscarinic Receptor Is Required for Optimal Adaptive Immunity to Helminth and Bacterial Infection. *PLOS Pathog*. 2015; 11:e1004636. [PubMed: 25629518]
- Dhawan S, Cailotto C, Harthoorn LF, de Jonge WJ. Cholinergic signalling in gut immunity. *Life Sci*. 2012; 91:1038–1042. [PubMed: 22580288]
- Dhawan S, Hiemstra IH, Verseijden C, Hilbers FW, Te Velde AA, Willemsen LEM, Stap J, den Haan JM, de Jonge WJ. Cholinergic receptor activation on epithelia protects against cytokine-induced barrier dysfunction. *Acta Physiol Oxf Engl*. 2015; 213:846–859.
- Dhawan S, Palma GD, Willemze RA, Hilbers FW, Verseijden C, Luyer MD, Nuding S, Wehkamp J, Souwer Y, de Jong EC, et al. Acetylcholine-producing T cells in the intestine regulate antimicrobial peptide expression and microbial diversity. *Am J Physiol - Gastrointest Liver Physiol*. 2016; 311:G920–G933. [PubMed: 27514477]
- Duerr JS, Han H-P, Fields SD, Rand JB. Identification of major classes of cholinergic neurons in the nematode *Caenorhabditis elegans*. *J Comp Neurol*. 2008; 506:398–408. [PubMed: 18041778]
- Erickson CS, Lee SJ, Barlow-Anacker AJ, Druckenbrod NR, Epstein ML, Gosain A. Appearance of cholinergic myenteric neurons during enteric nervous system development: comparison of different ChAT fluorescent mouse reporter lines. *Neurogastroenterol Motil Off J Eur Gastrointest Motil Soc*. 2014; 26:874–884.
- Foong JPP, Tough IR, Cox HM, Bornstein JC. Properties of cholinergic and non-cholinergic submucosal neurons along the mouse colon. *J Physiol*. 2014; 592:777–793. [PubMed: 24344165]
- Gautron L, Rutkowski JM, Burton MD, Wei W, Wan Y, Elmquist JK. Neuronal and nonneuronal cholinergic structures in the mouse gastrointestinal tract and spleen. *J Comp Neurol*. 2013; 521:3741–3767. [PubMed: 23749724]
- Gilani AH, Ghayur MN, Saify ZS, Ahmed SP, Choudhary MI, Khalid A. Presence of cholinomimetic and acetylcholinesterase inhibitory constituents in betel nut. *Life Sci*. 2004; 75:2377–2389. [PubMed: 15350815]
- Grando SA, Kawashima K, Kirkpatrick CJ, Kummer W, Wessler I. Recent progress in revealing the biological and medical significance of the non-neuronal cholinergic system. *Int Immunopharmacol*. 2015; 29:1–7. [PubMed: 26362206]
- Harrington AM, Peck CJ, Liu L, Burcher E, Hutson JM, Southwell BR. Localization of muscarinic receptors M1R, M2R and M3R in the human colon. *Neurogastroenterol Motil Off J Eur Gastrointest Motil Soc*. 2010; 22:999–1008. e262–3.
- Head B, Aballay A. Recovery from an Acute Infection in *C. elegans* Requires the GATA Transcription Factor ELT-2. *PLoS Genet*. 2014; 10:e1004609. [PubMed: 25340560]
- Hirota CL, McKay DM. Cholinergic regulation of epithelial ion transport in the mammalian intestine. *Br J Pharmacol*. 2006; 149:463–479. [PubMed: 16981004]
- Hobert O. The neuronal genome of *Caenorhabditis elegans*. *WormBook*. 2013:1–106.
- Hooper, LV. Chapter 3 - Epithelial Cell Contributions to Intestinal Immunity. In: Alt, FW., editor. *Advances in Immunology*. Academic Press; 2015. p. 129-172.
- Hwang JM, Chang DJ, Kim US, Lee YS, Park YS, Kaang BK, Cho NJ. Cloning and functional characterization of a *Caenorhabditis elegans* muscarinic acetylcholine receptor. *Receptors Channels*. 1999; 6:415–424. [PubMed: 10635059]
- Iraozqui JE, Ng A, Xavier RJ, Ausubel FM. Role for beta-catenin and HOX transcription factors in *Caenorhabditis elegans* and mammalian host epithelial-pathogen interactions. *Proc Natl Acad Sci U S A*. 2008; 105:17469–17474. [PubMed: 18981407]

- Irazaqui JE, Troemel ER, Feinbaum RL, Luhachack LG, Cezairliyan BO, Ausubel FM. Distinct pathogenesis and host responses during infection of *C. elegans* by *P. aeruginosa* and *S. aureus*. *PLoS Pathog.* 2010; 6:e1000982. [PubMed: 20617181]
- Jeremias IC, Victorino VJ, Barbeiro HV, Kubo SA, Prado CM, Lima TM, Soriano FG. The Role of Acetylcholine in the Inflammatory Response in Animals Surviving Sepsis Induced by Cecal Ligation and Puncture. *Mol Neurobiol.* 2016; 53:6635–6643. [PubMed: 26637327]
- Jönsson M, Norrgård O, Forsgren S. Presence of a marked nonneuronal cholinergic system in human colon: study of normal colon and colon in ulcerative colitis. *Inflamm Bowel Dis.* 2007; 13:1347–1356. [PubMed: 17663429]
- Karin M, Clevers H. Reparative inflammation takes charge of tissue regeneration. *Nature.* 2016; 529:307–315. [PubMed: 26791721]
- Khan MRI, Anisuzzaman ASM, Semba S, Ma Y, Uwada J, Hayashi H, Suzuki Y, Takano T, Ikeuchi H, Uchino M, et al. M1 is a major subtype of muscarinic acetylcholine receptors on mouse colonic epithelial cells. *J Gastroenterol.* 2013; 48:885–896. [PubMed: 23242454]
- Khan RI, Yazawa T, Anisuzzaman ASM, Semba S, Ma Y, Uwada J, Hayashi H, Suzuki Y, Ikeuchi H, Uchino M, et al. Activation of focal adhesion kinase via M1 muscarinic acetylcholine receptor is required in restitution of intestinal barrier function after epithelial injury. *Biochim Biophys Acta.* 2014; 1842:635–645. [PubMed: 24365239]
- Kini AT, Thangaraj KR, Simon E, Shivappagowdar A, Thiagarajan D, Abbas S, Ramachandran A, Venkatraman A. Aberrant Niche Signaling in the Etiopathogenesis of Ulcerative Colitis: *Inflamm. Bowel Dis.* 2015:1.
- Koslowski MJ, Kübler I, Chamaillard M, Schaeffeler E, Reinisch W, Wang G, Beisner J, Tegl A, Peyrin-Biroulet L, Winter S, et al. Genetic variants of Wnt transcription factor TCF-4 (TCF7L2) putative promoter region are associated with small intestinal Crohn's disease. *PLoS ONE.* 2009; 4:e4496. [PubMed: 19221600]
- Koslowski MJ, Teltschik Z, Beisner J, Schaeffeler E, Wang G, Kübler I, Gersemann M, Cooney R, Jewell D, Reinisch W, et al. Association of a functional variant in the Wnt co-receptor LRP6 with early onset ileal Crohn's disease. *PLoS Genet.* 2012; 8:e1002523. [PubMed: 22393312]
- Lackner MR, Kim SK. Genetic Analysis of the *Caenorhabditis elegans* MAP Kinase Gene *mpk-1*. *Genetics.* 1998; 150:103–117. [PubMed: 9725833]
- Lackner MR, Nurrish SJ, Kaplan JM. Facilitation of Synaptic Transmission by EGL-30 Gqα and EGL-8 PLCβ: DAG Binding to UNC-13 Is Required to Stimulate Acetylcholine Release. *Neuron.* 1999; 24:335–346. [PubMed: 10571228]
- Lehner B, Tischler J, Fraser AG. RNAi screens in *Caenorhabditis elegans* in a 96-well liquid format and their application to the systematic identification of genetic interactions. *Nat Protoc.* 2006; 1:1617–1620. [PubMed: 17406454]
- Lualien RJ, Bakowski MA, Troemel ER. Characterization of Microsporidia-Induced Developmental Arrest and a Transmembrane Leucine-Rich Repeat Protein in *Caenorhabditis elegans*. *PLoS ONE.* 2015:10.
- Mahoney TR, Luo S, Nonet ML. Analysis of synaptic transmission in *Caenorhabditis elegans* using an aldicarb-sensitivity assay. *Nat Protoc.* 2006; 1:1772–1777. [PubMed: 17487159]
- Matera MG, Rogliani P, Cazzola M. Muscarinic receptor antagonists for the treatment of chronic obstructive pulmonary disease. *Expert Opin Pharmacother.* 2014; 15:961–977. [PubMed: 24669979]
- Matteoli G, Boeckxstaens GE. The vagal innervation of the gut and immune homeostasis. *Gut.* 2013; 62:1214–1222. [PubMed: 23023166]
- McGhee JD. The *C. elegans* intestine. *WormBook Online Rev. C Elegans Biol.* 2007:1–36.
- McLean LP, Smith A, Cheung L, Sun R, Grinchuk V, Vanuytsel T, Desai N, Urban JF, Zhao A, Raufman J-P, et al. Type 3 Muscarinic Receptors Contribute to Clearance of *Citrobacter rodentium*. *Inflamm Bowel Dis.* 2015; 21:1860–1871. [PubMed: 25985244]
- McMullan R, Anderson A, Nurrish S. Behavioral and immune responses to infection require Gαq-RhoA signaling in *C. elegans*. *PLoS Pathog.* 2012; 8:e1002530. [PubMed: 22359503]
- Melo JA, Ruvkun G. Inactivation of conserved *C. elegans* genes engages pathogen- and xenobiotic-associated defenses. *Cell.* 2012; 149:452–466. [PubMed: 22500807]

- Miller KG, Emerson MD, Rand JB. Gαq and diacylglycerol kinase negatively regulate the Gαq pathway in *C. elegans*. *Neuron*. 1999; 24:323–333. [PubMed: 10571227]
- Najibi M, Labeled SA, Visvikis O, Irazoqui JE. An Evolutionarily Conserved PLC-PKD-TFEB Pathway for Host Defense. *Cell Rep*. 2016; 15:1728–1742. [PubMed: 27184844]
- Oettgen P. Regulation of Vascular Inflammation and Remodeling by ETS Factors. *Circ Res*. 2006; 99:1159–1166. [PubMed: 17122446]
- O’rourke D, Baban D, Demidova M, Mott R, Hodgkin J. Genomic clusters, putative pathogen recognition molecules, and antimicrobial genes are induced by infection of *C. elegans* with *M. nematophilum*. *Genome Res*. 2006; 16:1005–1016. [PubMed: 16809667]
- Peng Z, Heath J, Drachenberg C, Raufman JP, Xie G. Cholinergic muscarinic receptor activation augments murine intestinal epithelial cell proliferation and tumorigenesis. *BMC Cancer*. 2013; 13:204. [PubMed: 23617763]
- Pereira L, Kratsios P, Serrano-Saiz E, Sheftel H, Mayo AE, Hall DH, White JG, LeBoeuf B, Garcia LR, Alon U, et al. A cellular and regulatory map of the cholinergic nervous system of *C. elegans*. *ELife*. 2015; 4:e12432. [PubMed: 26705699]
- Peterson LW, Artis D. Intestinal epithelial cells: regulators of barrier function and immune homeostasis. *Nat Rev Immunol*. 2014; 14:141–153. [PubMed: 24566914]
- Pfaffl MW. A new mathematical model for relative quantification in real-time RT-PCR. *Nucleic Acids Res*. 2001; 29:e45. [PubMed: 11328886]
- Pochini L, Scalise M, Galluccio M, Pani G, Siminovitch KA, Indiveri C. The human OCTN1 (SLC22A4) reconstituted in liposomes catalyzes acetylcholine transport which is defective in the mutant L503F associated to the Crohn’s disease. *Biochim Biophys Acta*. 2012; 1818:559–565. [PubMed: 22206629]
- Powell JR, Ausubel FM. Models of *Caenorhabditis elegans* infection by bacterial and fungal pathogens. *Methods Mol Biol Clifton NJ*. 2008; 415:403–427.
- Powell JR, Kim DH, Ausubel FM. The G protein-coupled receptor FSHR-1 is required for the *Caenorhabditis elegans* innate immune response. *Proc Natl Acad Sci U S A*. 2009; 106:2782–2787. [PubMed: 19196974]
- Profita M, Bonanno A, Siena L, Ferraro M, Montalbano AM, Pompeo F, Riccobono L, Pieper MP, Gjomarkaj M. Acetylcholine mediates the release of IL-8 in human bronchial epithelial cells by a NFκB/ERK-dependent mechanism. *Eur J Pharmacol*. 2008; 582:145–153. [PubMed: 18242599]
- Pujol N, Ewbank JJ, Link EM, Liu LX, Kurz CL, Alloing G, Tan MWW, Ray KP, Solari R, Johnson CD. A reverse genetic analysis of components of the Toll signaling pathway in *Caenorhabditis elegans*. *Curr Biol CB*. 2001; 11:809–821. [PubMed: 11516642]
- Qadota H, Inoue M, Hikita T, Köppen M, Hardin JD, Amano M, Moerman DG, Kaibuchi K. Establishment of a tissue-specific RNAi system in *C. elegans*. *Gene*. 2007; 400:166–173. [PubMed: 17681718]
- Rand JB. Acetylcholine. *WormBook Online Rev. C Elegans Biol*. 2007:1–21.
- Raufman J-P, Samimi R, Shah N, Khurana S, Shant J, Drachenberg C, Xie G, Wess J, Cheng K. Genetic Ablation of M3 Muscarinic Receptors Attenuates Murine Colon Epithelial Cell Proliferation and Neoplasia. *Cancer Res*. 2008; 68:3573–3578. [PubMed: 18483237]
- Rebecchi MJ, Pentylala SN. Structure, Function, and Control of Phosphoinositide-Specific Phospholipase C. *Physiol Rev*. 2000; 80:1291–1335. [PubMed: 11015615]
- Rössler OG, Henß I, Thiel G. Transcriptional response to muscarinic acetylcholine receptor stimulation: Regulation of Egr-1 biosynthesis by ERK, Elk-1, MKP-1, and calcineurin in carbachol-stimulated human neuroblastoma cells. *Arch Biochem Biophys*. 2008; 470:93–102. [PubMed: 18061571]
- Rubin GM, Yandell MD, Wortman JR, Gabor GL, Miklos Nelson CR, Hariharan IK, Fortini ME, Li PW, Apweiler R, et al. Comparative Genomics of the Eukaryotes. *Science*. 2000; 287:2204–2215. [PubMed: 10731134]
- Sales ME. Muscarinic receptors as targets for anti-inflammatory therapy. *Curr Opin Investig Drugs Lond Engl*. 2010; 11:1239–1245.
- Sarkar A, Lehto SM, Harty S, Dinan TG, Cryan JF, Burnet PWJ. Psychobiotics and the Manipulation of Bacteria–Gut–Brain Signals. *Trends Neurosci*. 2016; 39:763–781. [PubMed: 27793434]

- Sawa, H., Korswagen, HC. T.C. elegans R. Community. WormBook. 2013. Wnt signaling in *C. elegans*.
- Silva-García O, Valdez-Alarcón JJ, Baizabal-Aguirre VM. The Wnt/ β -catenin signaling pathway controls the inflammatory response in infections caused by pathogenic bacteria. *Mediators Inflamm.* 2014; 2014:310183. [PubMed: 25136145]
- Stahelin RV, Digman MA, Medkova M, Ananthanarayanan B, Rafter JD, Melowic HR, Cho W. Mechanism of Diacylglycerol-induced Membrane Targeting and Activation of Protein Kinase C δ . *J Biol Chem.* 2004; 279:29501–29512. [PubMed: 15105418]
- Steger KA, Avery L. The GAR-3 muscarinic receptor cooperates with calcium signals to regulate muscle contraction in the *Caenorhabditis elegans* pharynx. *Genetics.* 2004; 167:633–643. [PubMed: 15238517]
- Timmons L, Court DL, Fire A. Ingestion of bacterially expressed dsRNAs can produce specific and potent genetic interference in *Caenorhabditis elegans*. *Gene.* 2001; 263:103–112. [PubMed: 11223248]
- Tracey KJ. Approaching the Next Revolution? Evolutionary Integration of Neural and Immune Pathogen Sensing and Response. *Cold Spring Harb Perspect Biol.* 2014
- Tsoyi K, Geldart AM, Christou H, Liu X, Chung SW, Perrella MA. Elk-3 is a KLF4-regulated gene that modulates the phagocytosis of bacteria by macrophages. *J Leukoc Biol.* 2015; 97:171–180. [PubMed: 25351511]
- Vaishnav S, Yamamoto M, Severson KM, Ruhn KA, Yu X, Koren O, Ley R, Wakeland EK, Hooper LV. The antibacterial lectin RegIII γ promotes the spatial segregation of microbiota and host in the intestine. *Sci N Y NY.* 2011; 334:255–258.
- Verbout, NG., Jacoby, DB. Muscarinic Receptor Agonists and Antagonists: Effects on Inflammation and Immunity. In: Fryer, AD,Christopoulos, A., Nathanson, NM., editors. *Muscarinic Receptors.* Berlin, Heidelberg: Springer Berlin Heidelberg; 2012. p. 403-427.
- Wess J, Eglén RM, Gautam D. Muscarinic acetylcholine receptors: mutant mice provide new insights for drug development. *Nat Rev Drug Discov.* 2007; 6:721–733. [PubMed: 17762886]
- White JG, Southgate E, Thomson JN, Brenner S. The structure of the nervous system of the nematode *Caenorhabditis elegans*. *Philos Trans R Soc Lond B Biol Sci.* 1986; 314:1–340. [PubMed: 22462104]
- Wong D, Bazopoulou D, Pujol N, Tavernarakis N, Ewbank JJ. Genome-wide investigation reveals pathogen-specific and shared signatures in the response of *Caenorhabditis elegans* to infection. *Genome Biol.* 2007; 8:R194. [PubMed: 17875205]
- Xu Z, Dziarski R, Wang Q, Swartz K, Sakamoto KM, Gupta D. Bacterial peptidoglycan-induced tnf- α transcription is mediated through the transcription factors Egr-1, Elk-1, and NF-kappaB. *J Immunol Baltim Md 1950.* 2001; 167:6975–6982.
- Yoo BB, Mazmanian SK. The Enteric Network: Interactions between the Immune and Nervous Systems of the Gut. *Immunity.* 2017; 46:910–926. [PubMed: 28636959]
- Zhao C-M, Hayakawa Y, Kodama Y, Muthupalani S, Westphalen CB, Andersen GT, Flatberg A, Johannessen H, Friedman RA, Renz BW, et al. Denervation suppresses gastric tumorigenesis. *Sci Transl Med.* 2014; 6:250ra115-250ra115.

Highlights

- Acetylcholine regulates transcriptional host defense in intestinal epithelial cells
- Acetylcholine activates muscarinic and Wnt signaling in the intestine
- Transcription factor *lin-1* (ELK) links muscarinic and Wnt pathways by Wnt induction

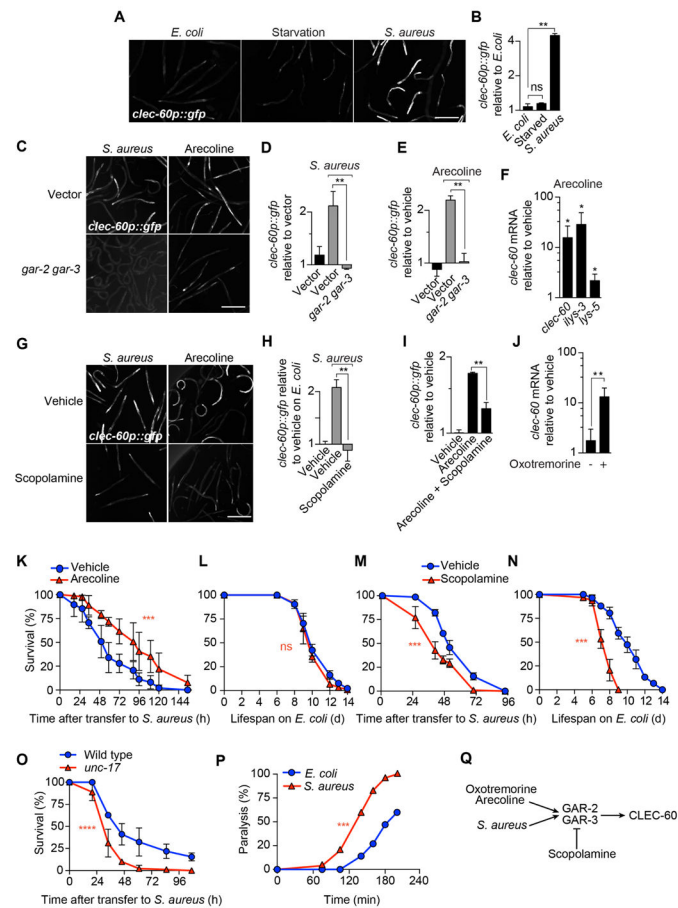


Figure 1. Muscarinic receptors control host defense against infection

(A) Epifluorescence micrographs of animals expressing GFP from the *clec-60* promoter (*clec-60p::gfp*) after 8 h of feeding on *E. coli*, starvation, or infection with *S. aureus*. (B) Quantitative analysis of (A). Data are mean \pm SEM (two independent biological replicates, n = 50 per condition). ** $p < 0.01$ (see **STAR Methods** for description of statistical methods). ns, not significant. (C) Representative epifluorescence micrographs of *clec-60p::gfp* animals that were reared on *E. coli* carrying empty vector (top row) or *gar-2*, *gar-3* double RNAi (bottom row), and subsequently infected 16 h with *S. aureus* (left column) or treated for 16 h with 5 mM arecoline (right column). (D) Quantitative analysis of (C). Data are mean \pm SEM (two independent biological replicates, n = 50 per condition). (E) *clec-60p::gfp* expression after 16 h incubation of uninfected animals with 5 mM arecoline. Data are mean \pm SEM (at least two independent biological replicates, n = 50 per condition). (F) qRT-PCR of *clec-60*, *ilys-3*, and *lys-5* in wild type animals incubated with 5 mM arecoline for 8 h, normalized to vehicle treated animals. Data are mean \pm SEM (three independent biological replicates, n = 3,000 per condition). * $p < 0.05$. (G) Representative epifluorescence micrographs of *clec-60p::gfp* animals that were treated with vehicle (top row) or 5 mM scopolamine (bottom row), during 16 h infection with *S. aureus* (left column) or treated with 5 mM arecoline for 16 h (right column). (H) Quantitative analysis of infection in (G). (I) Quantitative analysis of scopolamine treatment in (G). Data are mean \pm SEM (at least two independent biological replicates, n = 50 per condition). (J) qRT-PCR of

clec-60 in wild type animals treated with 1 mM oxotremorine for 8 h. Results are normalized to vehicle-treated animals. Data are mean \pm SEM (three independent biological replicates, n = 3,000 per condition). **(K)** Survival of wild type animals, treated with vehicle or 1 mM arecoline for 24 h prior to infection. Results are representative of 2 independent biological replicates. *** $p < 0.001$. **(L)** Lifespan of wild type animals treated with vehicle or 1 mM arecoline for 24 h before transfer to *E. coli* OP50. Results are representative of 2 independent biological replicates. ns, $p > 0.05$. **(M)** Survival of wild type animals, treated with vehicle or 1 mM scopolamine during the entire course of infection. Results are representative of 2 independent biological replicates. **(N)** Lifespan of wild type animals on *E. coli* OP50, treated with vehicle or 1 mM scopolamine. Results are representative of 2 independent biological replicates. **(O)** Survival of wild type and *unc-17* mutant animals infected with *S. aureus*. Results are representative of 2 independent biological replicates. **(P)** Aldicarb paralysis assays of infected and uninfected animals. Results are representative of at least 3 independent biological replicates. **(Q)** Schematic summary of results. Scale bars, 0.6 mm. Also see Figure S1.

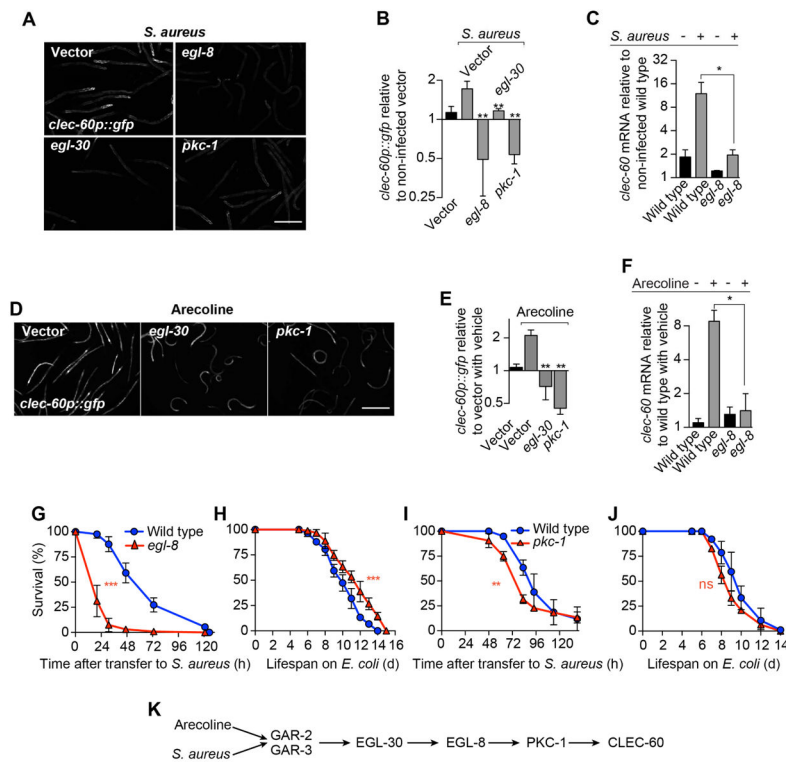


Figure 2. Gaq, phospholipase C β , and protein kinase C η function downstream of muscarinic receptors

(A) Epifluorescence micrographs of *clec-60p::gfp* animals reared on *E. coli* carrying empty vector or RNAi against *egl-8*, *pkc-1*, or *egl-30*, and subsequently infected with *S. aureus* for 16 h. (B) Quantitative analysis of (A). Data are mean \pm SEM (at least 2 independent biological replicates, n = 50 per condition). (C) qRT-PCR of *clec-60* in wild type animals and *egl-8* mutants after 8 h *S. aureus* infection. Results are normalized to non-infected wild type. Data are mean \pm SEM (three independent biological replicates, n = 3,000 per condition). (D) Representative epifluorescence micrographs of *clec-60p::gfp* animals reared on *E. coli* carrying empty vector or RNAi against *egl-30* or *pkc-1*, and subsequently treated with 5 mM arecoline for 16 h. (E) Quantitative analysis of (D). Data are mean \pm SEM (at least two independent biological replicates, n = 50 per condition). (F) qRT-PCR of *clec-60* in wild type and *egl-8* mutant animals after 8 h treatment with 1 mM arecoline. Results are normalized to vehicle treated wild type. Data are mean \pm SEM (three independent biological replicates, n = 3,000 per condition). (G) Survival of wild type and *egl-8* mutant animals infected with *S. aureus*. Results are representative of 2 independent biological replicates. (H) Lifespan of wild type and *egl-8* mutant animals on *E. coli* OP50. Results are representative of 2 independent biological replicates. (I) Survival of wild type and *pkc-1* mutant animals infected with *S. aureus*. Results are representative of 2 independent biological replicates. (J) Lifespan of wild type and *pkc-1* mutant animals on *E. coli* OP50. Results are representative of 2 independent biological replicates. ns, $p > 0.05$. (K) Schematic summary of results. Scale bars, 0.6 mm.

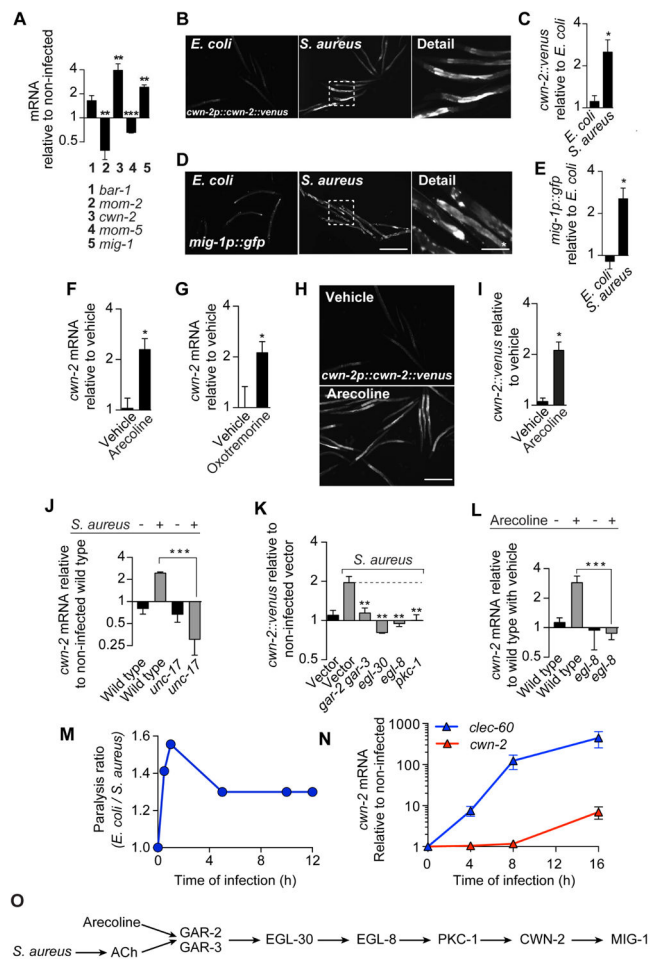


Figure 3. Infection and acetylcholine induce Wnt ligand in the intestinal epithelium
(A) qRT-PCR of Wnt pathway genes in wild type animals after 16 h *S. aureus* infection. Results are normalized to wild type animals fed on *E. coli* OP50. Data are mean \pm SEM (three independent biological replicates, n = 3,000 per condition). **(B)** Representative epifluorescence micrographs of animals expressing Venus-tagged CWN-2 protein from the *cwn-2* promoter (*cwn-2p::cwn-2::venus*) after 24 h of feeding on *E. coli* or infection with *S. aureus*. **(C)** Quantitative analysis of (B). Results are normalized to *E. coli* controls. Data are mean \pm SEM (two independent biological replicates, n = 50 per condition). **(D)** Representative epifluorescence micrographs of animals expressing GFP from the *mig-1* promoter (*mig-1p::gfp*) after 24 h of feeding on *E. coli* or infection with *S. aureus*. **(E)** Quantitative analysis of (D). Results are normalized to *E. coli* controls. Data are mean \pm SEM (two independent biological replicates, n = 50 per condition). **(F)** qRT-PCR of *cwn-2* in wild type animals after 16 h treatment with 5 mM arecoline. Data are mean \pm SEM (three independent biological replicates, n = 3,000 per condition). **(G)** Same as in (F), but after 16 h treatment with 1 mM oxotremorine. **(H)** Representative epifluorescence micrographs of *cwn-2p::cwn-2::venus* animals after 24 h treatment with 5 mM arecoline. **(I)** Quantitative analysis of (H). Results are normalized to vehicle controls. Data are mean \pm SEM (two independent biological replicates, n = 50 per condition). **(J)** qRT-PCR of *cwn-2* in wild type

animals and *unc-17* mutants infected with *S. aureus* for 16 h. Results are normalized to *E. coli* wild type control. Data are mean \pm SEM (three independent biological replicates, n 3,000 per condition). **(K)** CWN-2::Venus expression after 24 h *S. aureus* infection, in animals reared on *E. coli* carrying empty vector or RNAi against *gar-2* and *gar-3*, *egl-30*, *egl-8*, or *pkc-1*. Data are mean \pm SEM (two independent biological replicates, n 50 per condition). Results are normalized to *E. coli* empty vector control. **(L)** qRT-PCR of *cwn-2* in wild type and *egl-8* mutant animals after 16 h treatment with 5 mM arecoline. Results are normalized to vehicle-treated wild type. Data are mean \pm SEM (three independent biological replicates, n 3,000 per condition). **(M)** Time course of aldicarb paralysis. Data are the ratio of paralysis frequencies of infected animals v. *E. coli* controls at each time point. Results are representative of 3 independent biological replicates. **(N)** Time course of *cwn-2* and *clec-60* mRNA induction. Data are *cwn-2* or *clec-60* expression in infected animals relative to *E. coli* controls. Mean \pm SEM (three independent biological replicates, n 3,000 per condition). **(O)** Schematic summary of results. Scale bars, 0.6 mm. Scale bars with *, 0.2 mm.

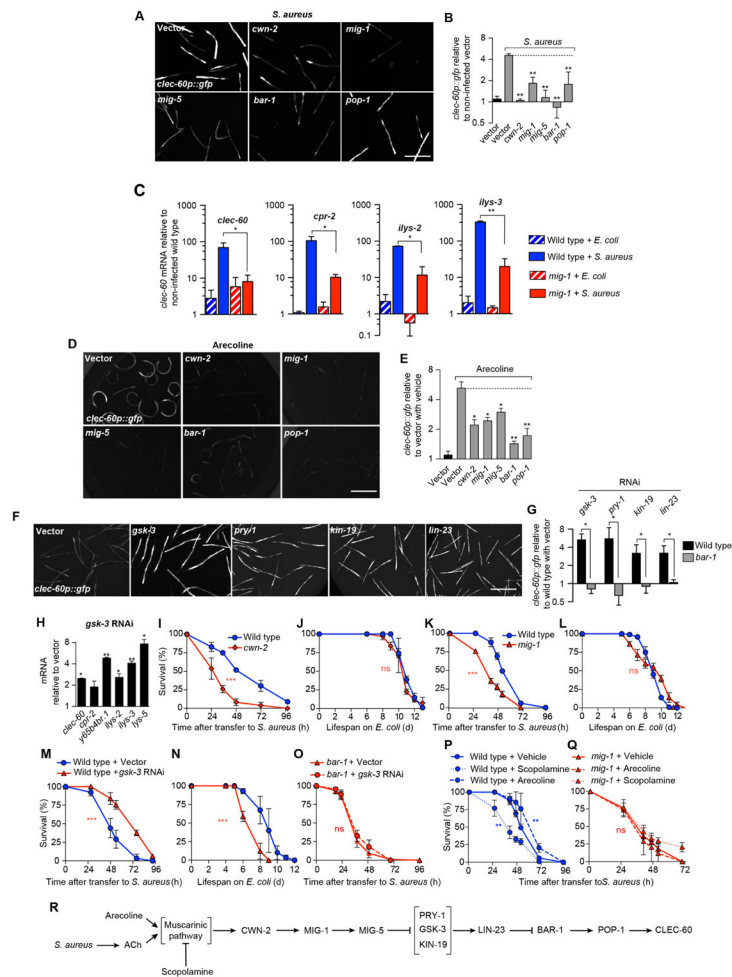


Figure 4. Canonical Wnt signaling is necessary and sufficient for host defense gene induction (A) Representative epifluorescence micrographs of *clec-60p::gfp* animals reared on *E. coli* carrying empty vector or RNAi against *cwn-2*, *mig-1*, *mig-5*, *bar-1*, or *pop-1*, and subsequently infected with *S. aureus* for 16 h. (B) Quantitative analysis of (A). Data are mean \pm SEM (at least two independent biological replicates, n = 50 per condition). (C) qRT-PCR of *clec-60*, *cpr-2*, *ilys-2*, and *ilys-3* in wild type and *mig-1* mutant animals after 8 h *S. aureus* infection. Results are normalized to *E. coli*-fed wild type. Data are mean \pm SEM (three independent biological replicates, n = 3,000 per condition). (D) Representative epifluorescence micrographs of *clec-60p::gfp* animals reared on *E. coli* carrying empty vector or RNAi against *cwn-2*, *mig-1*, *mig-5*, *bar-1*, or *pop-1*, and subsequently treated with 5 mM arecoline for 16 h. (E) Quantitative analysis of (D). Results are normalized to non-treated wild type animals. Data are mean \pm SEM (at least 2 independent biological replicates, n = 50 per condition). (F) Representative epifluorescence micrographs of *clec-60p::gfp* animals reared on *E. coli* carrying empty vector or RNAi against *gsk-3*, *pry-1*, *kin-19*, or *lin-23*. (G) Quantitative analysis of (F). Results are normalized to wild type animals on empty vector. Data are mean \pm SEM (two independent biological replicates, n = 50 per condition). (H) qRT-PCR of antimicrobial genes in wild type animals on *gsk-3* RNAi. Results are normalized to empty vector controls. Data are mean \pm SEM (three independent

biological replicates, n = 3000 per condition). **(I)** Survival of wild type and *cwn-2* mutant animals infected with *S. aureus*. Results are representative of 2 independent biological replicates. **(J)** Lifespan of wild type and *cwn-2* mutant animals fed *E. coli* OP50. Results are representative of 2 independent biological replicates. **(K)** Survival of wild type and *mig-1* mutant animals infected with *S. aureus*. Results are representative of 2 independent biological replicates. **(L)** Lifespan of wild type and *mig-1* mutant animals fed *E. coli* OP50. Results are representative of 2 independent biological replicates. **(M)** Survival of wild type animals grown on empty vector or *gsk-3* RNAi, and subsequently infected with *S. aureus*. Results are representative of 2 independent biological replicates. **(N)** Lifespan of animals treated as in (M), but transferred to *E. coli* OP50 after RNAi. Results are representative of 2 independent biological replicates. **(O)** Survival of *bar-1* mutant animals treated as in (M). Results are representative of 2 independent biological replicates. **(P)** Survival of wild type animals treated with vehicle, 1 mM arecoline, or 1 mM scopolamine. Arecoline treatment was 24 h prior to infection and scopolamine was applied during infection. Results are representative of 2 independent biological replicates. **(Q)** Survival of *mig-1* mutant animals, treated as in (P). Results are representative of 2 independent biological replicates. **(R)** Schematic summary of results. Scale bars, 0.6 mm. Also see Figure S2.

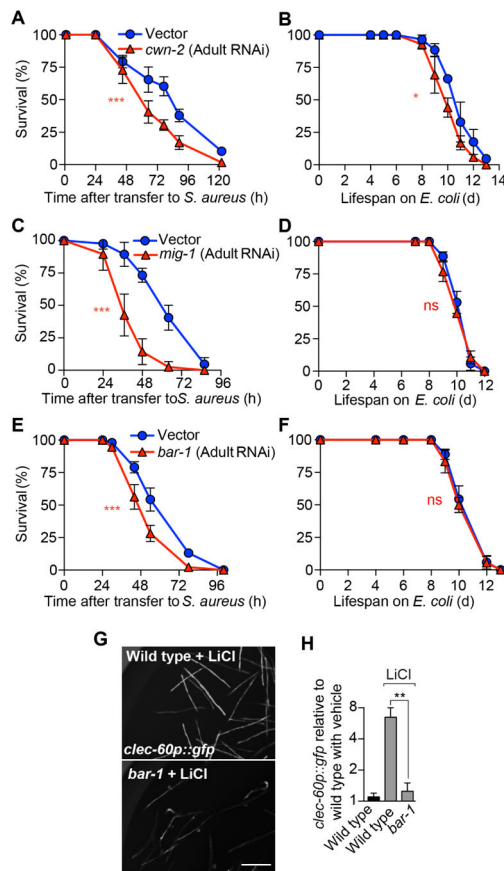


Figure 5. Wnt signaling functions post-developmentally for host defense

(A, B) Wild type animals were subjected to RNAi against *cwn-2*, starting at the late L4 or young adult stage. Following RNAi, animals were infected with *S. aureus* (A), or transferred to *E. coli* OP50 plates (B). Results are representative of 2 independent biological replicates. (C, D) Same as in (A, B), but performing RNAi against *mig-1*. Results are representative of 2 independent biological replicates. (E, F) Same as in (A, B), but performing RNAi against *bar-1*. Results are representative of 2 independent biological replicates. (G) Representative epifluorescence micrographs of *clec-60p::gfp* animals reared on *E. coli* carrying empty vector or RNAi against *bar-1*, and subsequently treated with 100 mM LiCl for 16 h. (H) Quantitative analysis of (G). Results are normalized to vehicle-treated wild type animals. Data are mean \pm SEM (2–3 independent biological replicates, n = 50 per condition). Scale bars, 0.6 mm.

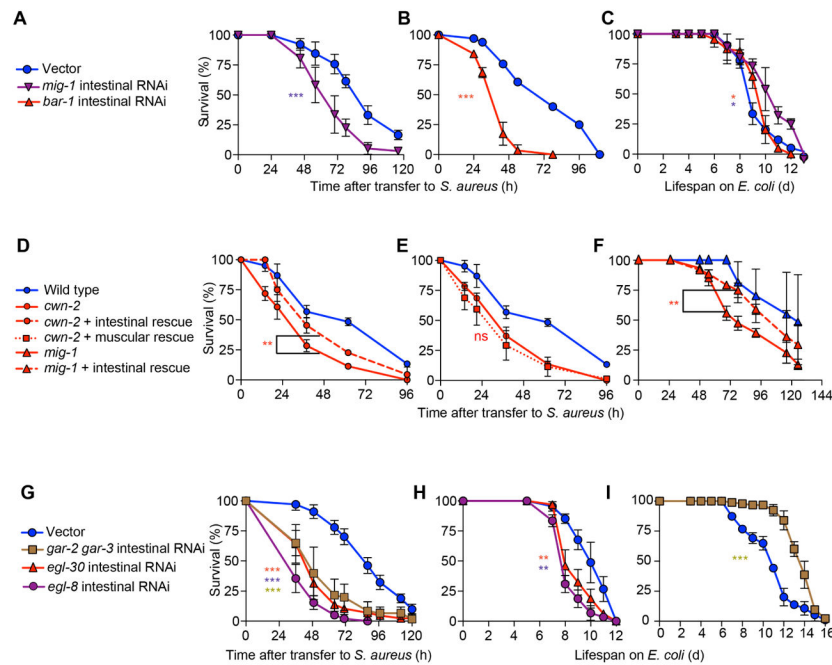


Figure 6. Muscarinic and Wnt signaling function in the intestinal epithelium

(A) Survival of MGH167 animals subjected to RNAi against *mig-1* until young adulthood, and subsequently infected with *S. aureus*. Results are representative of 2 independent biological replicates. (B) Same as in (A), but performing RNAi against *bar-1*. (C) Lifespan on *E. coli* OP50 of animals treated as in (A, B). Results are representative of 2 independent biological replicates. (D) Survival of wild type, *cwn-2(ok895)*, and *cwn-2(ok895)* mutants expressing wild type *cwn-2* in the intestinal epithelium. Results are representative of 2 independent biological replicates. (E) Survival of wild type, *cwn-2(ok895)* mutants, and *cwn-2* mutants expressing wild type *cwn-2* in the body wall muscle. (F) Survival of wild type, *mig-1(e1787)* mutants, and *mig-1(e1787)* mutants expressing wild type *mig-1* in the intestinal epithelium. Results are representative of 2 independent biological replicates. (G) Survival of MGH167 animals subjected to RNAi against *gar-2* and *gar-3*, *egl-30*, and *egl-8* until young adulthood, and subsequently infected with *S. aureus*. Results are representative of 2 independent biological replicates. (H, I) Lifespan on *E. coli* OP50 of animals treated with RNAi as in (G). Results are representative of 2 independent biological replicates. Also see Figure S6.

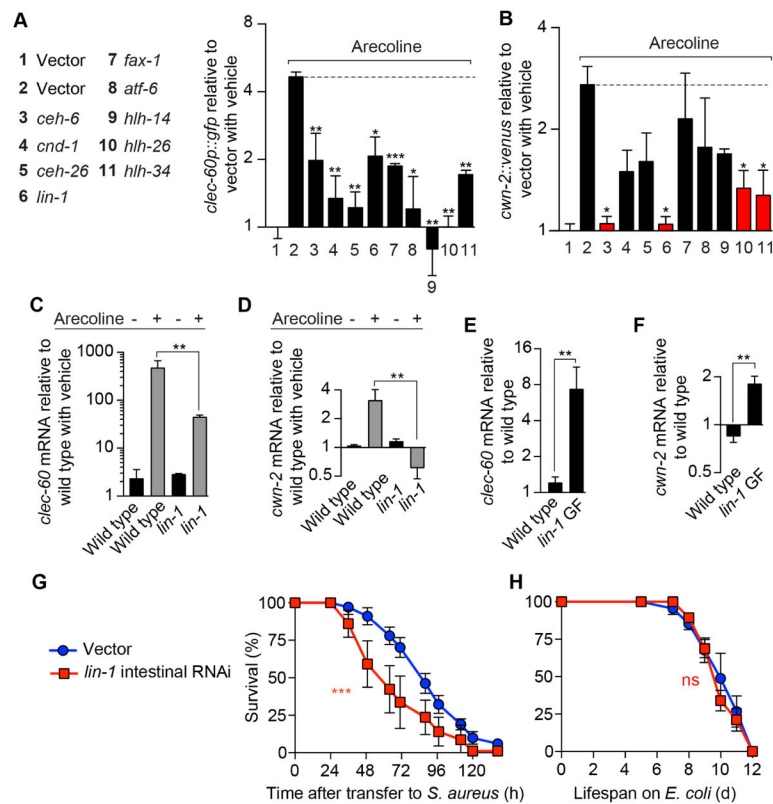


Figure 7. Transcription factors that link muscarinic and Wnt signaling

(A) Quantification of GFP expression in *clec-60p::gfp* animals subjected to RNAi against the indicated transcription factor genes, and subsequently treated with 5 mM arecoline for 16 h. Data are mean \pm SEM (2 independent biological replicates, n = 50 per condition). Results are normalized to vehicle-treated empty vector control. (B) Quantification of Venus expression in *cwn-2p::cwn-2::venus* animals treated with RNAi as in (A) and subsequently with 5 mM arecoline for 24 h. Data are mean \pm SEM (2 independent biological replicates, n = 50 per condition). Results are normalized to vehicle-treated empty vector control. (C) qRT-PCR of *clec-60* in wild type and *lin-1* null mutant animals treated with 5 mM arecoline for 8 h. Results are normalized to vehicle-treated wild type control. Data are mean \pm SEM (3 independent biological replicates, n = 3,000 per condition). (D) qRT-PCR of *cwn-2* in the same animals as in (C), treated with 5 mM arecoline for 16 h. (E) qRT-PCR of *clec-60* in *E. coli*-fed wild type and *lin-1* gain of function (GF) mutant animals. Results are normalized to wild type. Data are mean \pm SEM (3 independent biological replicates, n = 3,000 per condition). (F) qRT-PCR of *cwn-2* in the same animals as in (E). (G) MGH167 animals subjected to RNAi against *lin-1* until young adulthood, and subsequently infected with *S. aureus*. Results are representative of 2 independent biological replicates. (H) Lifespan of MGH167 animals treated as in (G), but placed on *E. coli* OP50. Also see Figure S5.